# Modification of Computer-Aided Modelling Input Data Based on Medium-Scale Fire Tests of Wooden Beams

Dominik Spilak [a,*] Katarina Dubravska [a] Andrea Majlingova [a] Cong Jin,[b] Qiang Xu,[c] and Lin Jiang [c]

* *Corresponding author: xspilakd@is.tuzvo.sk*

*DOI: 10.15376/biores.20.1.1230-1250*

## GRAPHICAL ABSTRACT

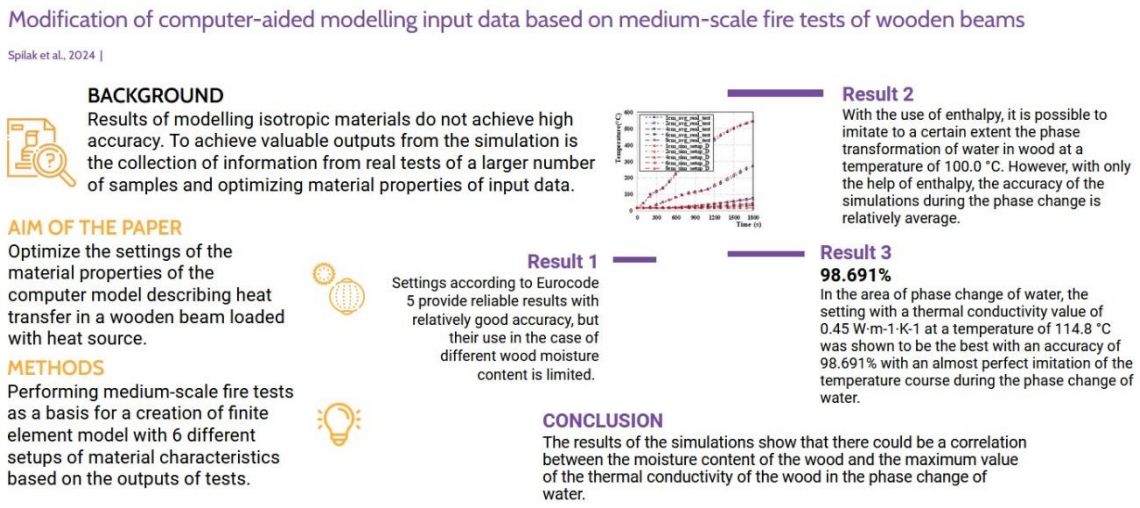

# Modification of Computer-Aided Modelling Input Data Based on Medium-Scale Fire Tests of Wooden Beams

Dominik Spilak [a,*] Katarina Dubravska [a] Andrea Majlingova [a] Cong Jin,[b] Qiang Xu,[c] and Lin Jiang [c]

The aim of the paper was to optimize the settings of the material properties of a computer model describing heat transfer in a wooden beam exposed to thermal loading from a porcelain radiation panel. The methodology was based on performing medium-scale fire tests as a basis for a creation of finite element model with 6 different setups of material characteristics based on the outputs of tests. When adjusting the settings, the T-history method was used to determine a beginning and end of a phase change of the water content in the wood, a thermal conductivity was adjusted based on a density and a moisture content, and enthalpy was used instead of a specific heat. The results of the simulations were compared with the real medium-scale fire tests, which showed the importance of adjusting the input data. Based on the T-history method, the setting with a thermal conductivity value of 0.35 $W \cdot m^{-1} \cdot K^{-1}$ at a temperature of 114.8 °C was shown to be the best, with a coefficient of determination 98.7%.The results of the simulations showed that there could be a correlation between the moisture content of the wood and the maximum value of the thermal conductivity of the wood in the phase change of water.

*DOI: 10.15376/biores.20.1.1230-1250*

*Keywords: Wood; Finite element model; Input data; Material characteristics*

*Contact information: a: Department of Fire Protection, Faculty of Wood Sciences and Technology, Technical University in Zvolen, 960 01 Zvolen, Slovakia; b: Nanjing University of Science and Technology, School of Computer Science and Engineering, 200 Xiao Ling Wei, 210014 Nanjing, P. R. China; c: Nanjing University of Science and Technology, School of Mechanical Engineering, 200 Xiao Ling Wei, 210014 Nanjing, P. R. China; * Corresponding author: xspilakd@is.tuzvo.sk*

## INTRODUCTION

Currently, computer modeling based on finite element analysis (FEA) is increasingly involved in the design of buildings and the material design of structures, which provides several advantages. FEA is used to perform models, simulations, and provide the user with an idea of how the material or structure will probably behave under a certain load. The basic condition for comparing results from experimental tests or practice with results from FEA is the quality of the input data. As stated by Wald *et al*. (2017), one of the disadvantages of FEA-based software is the difficult availability of input data, especially material and fire characteristics, which can burden the output data with a significant error. These are drawn from standards or other research literature.

In the case of modeling the behavior of homogeneous materials subjected to thermal loading, FEA and entering material properties are simple. Samples made of isotropic material do not differ from each other. Thus, model preparation building, and simulation setup are simple. The results are of high accuracy and are relatively easy replicable. In the case of modeling the behavior of anisotropic materials such as wood,

material properties that differ not only in different directions but also in one direction, are a fundamental problem. Moisture content is also an important factor, which completely changes the properties of wood (Malaga-Tobola *et al*. 2019; Hu *et al*. 2023). Therefore, the results of modeling isotropic materials do not provide high accuracy. The key to achieving valuable outputs from the simulation is the collection of information from real fire tests using a larger number of samples. The prepared model is subsequently validated with the average values obtained from real fire tests. In this way, it is possible to achieve the most accurate results in the simulations of the behavior of anisotropic materials exposed to thermal loading.

The aim of the paper was to optimize the settings of the material properties of the computer model describing heat transfer in a wooden beam loaded with heat source. The basis for achieving accurate outputs from simulations of heat conduction in wood and the process of the formation of a charred layer is correctly entered input data relating primarily to the material characteristics of wood. The key variables are thermal conductivity, heat capacity, and density (Bartlett *et al*. 2019). All previous properties of wood depend on temperature.

The thermal conductivity of wood has been investigated by many authors. Naser (Naser 2019) and Maraveas *et al*. (2015) compared the measured values of the thermal conductivity of different wood species exposed to thermal load from several authors (Janssens and White 1994; Frangi 2001; EN 1995-1-2 2004; Maciulaitis *et al*. 2012; Wald *et al*. 2017; Kamenická *et al*. 2018; Bartlett *et al*. 2019; Kmiecik 2019; Malaga-Tobola *et al*. 2019; Naser 2019; Hu *et al*. 2023). They pointed out the high dispersion of the measured values caused by different measurement procedures and the diversity of the measured wood species. It is therefore impractical to use the values given in EN 1995-1-2 (2004), for numerical calculations, because there is little chance for accurate results.

The thermal conductivity of wood depends on its density, moisture content, and fibre direction. According to Friquin (2011) and Peng *et al*. (2011) thermal conductivity is greater parallel to the fibres than perpendicular to them. Çavuş *et al*. (2019) investigated the thermal conductivity of 31 different wood species. Thermal conductivity varied from 0.090 to 0.197 $W \cdot m^{-1} \cdot K^{-1}$ and the highest thermal conductivity was obtained for oak with density 0.841 $g \cdot cm^{-3}$ and the lowest for Canadian poplar with density 0.340 $g \cdot cm^{-3}$. They obtained a linear relation between wood density and thermal conductivity shown in Eq. 1:

$$y = 4.2401 \times x - 0.0036 \quad (1)$$

where $y$ is the density of the wood and $x$ is the thermal conductivity. Jang and Kang (2022) investigated the effects of density on thermal conductivity in samples of 15 woods. Consistent with previous study, thermal conductivity was found to increase with density. According to research wood with lower density commonly had lower thermal conductivity, consequently resulting in a faster temperature rise at the surface, by reason of pyrolyzing and charring start earlier. Conversely, higher density of wood had higher through-thickness temperatures, and it pyrolyzed faster thanks to shallower thermal gradients (Bartlett *et al*. 2019).

Moisture content affects the process of heat transport in wood in several ways. Amel *et al*. (2016) in their study demonstrated the effect of moisture content on the thermal conductivity values of wood. The results showed that an increase in the moisture content of the samples leads to an increase in the value of the thermal conductivity of the wood. Krišťák *et al*. (2019) reached a similar conclusion and demonstrated different values of thermal conductivity of wood depending on moisture content. Vololonirina *et al*. (2014)

showed that changes in thermal conductivity depending on moisture content had a visible linear trend. Some authors investigated the effect of moisture content on the thermal conductivity of wood and wood materials and found a relatively linear relationship (Mvondo *et al*. 2020). For other authors, thermal conductivity increased with moisture content according to the equation of the second order with pronounced curvature depending on the material (Zvicevicius *et al*. 2019).

Despite the considerable dispersion of the thermal conductivity of different woods and wood materials depending on the moisture content, it is evident that the thermal conductivity increases with an increase in the moisture content of the wood with a more or less visible linear trend (Špilák *et al.* 2022b) (Eq. 2),

$$\lambda_{\omega} = 0{,}0064 \cdot (\omega - \omega_0) + \lambda_{\omega_0} \quad (2)$$

where $\lambda_{\omega}$ is the thermal conductivity of wood at moisture content $\omega$ ($W \cdot m^{-1} \cdot K^{-1}$), $\omega$ is the wood moisture content (%), $\omega_0$ is the initial wood moisture content (%) and $\lambda_{\omega 0}$ is the initial wood thermal conductivity at moisture content $\omega_0$ ($W \cdot m^{-1} \cdot K^{-1}$). Equation 2 is valid only up to a temperature of 100.0 °C, when the phase change of the water contained in the wood occurs. After exceeding this temperature, wood moisture has no longer a significant effect on its thermal conductivity.

During the process of heating wood during a fire, the phase of water changes. This results in a state where the received energy is not used for heating wood, but mainly for changing the phase of water (Reszka and Torero 2008; Cachim and Franssen 2009; Cachim and Franssen 2010; Friquin 2011; Maraveas *et al*. 2015; Pecenko *et al*. 2015; Richter and Rein 2020; Spilák and Majlingová 2022; Spilák *et al*. 2022a; Hu *et al*. 2023; Rinta-Paavola *et al*. 2023). This is reflected in the temperature curves during fire tests of wood by equilibrating the temperature in the region around 100 °C for a certain time until all the water has evaporated from the wood (Frangi 2001). Moisture acts as a pyrolysis retarder as it absorbs heat and cools the wood. The higher the moisture content of the wood, the lower the temperature reached in the wood for the same supplied energy (Shen *et al*. 2007; Cachim and Franssen 2009; Cachim and Franssen 2010; Friquin 2011; Maraveas *et al*. 2015; Richter and Rein 2020; Spilák and Majlingová 2022; Spilák *et al*. 2022a; Hu *et al*. 2023; Rinta-Paavola *et al*. 2023). Wood moisture content also affects the initial thermal conductivity of wood. Acuna-Alegri *et al*. (2018) state that with increased thermal conductivities, moisture content and temperature increased.

The charred layer is a black porous solid consisting predominantly of elemental carbon (Pinto *et al*. 2016). It consists of several layers. The charred cracked black layer has poorer thermal conductivity and thus slows down heat transfer to other layers (White and Dietenberger 2010). Some authors (Blass and Eurofortech 1995; Friquin 2011; Harper 2003) state that the thermal conductivity of the charred layer is lower than the thermal conductivity of intact wood. Su *et al*. (2019) state the fact that increasing the depth of the charred layer leads to improving a thermal insulating property.

Specific heat defines the amount of thermal energy to raise a unit mass of substance a single unit of temperature. Naser (2019) made a comparison of the measured values from different authors (Fredlund 1988; Fuller *et al*. 1992; Mehaffey *et al*. 1994; König 2000; Frangi 2001; EN 1995-1-2 2004) and pointed out the dispersion of the values, but it was not as significant as thermal conductivity. Almost all authors measured increased values of heat capacity in the range from 100.0 to 120.0 °C, which corresponded with the recommended values from EN 1995-1-2 (2004). The resulting jump is again caused by a change in the state of the water. Frangi (2001), as the only one of the mentioned authors,

states that the thermal capacity of wood is significantly higher than stated by EN 1995-1-2 (2004), while the dramatic increase in values started at 95.0 °C (1.73 kJ·kg$^{-1}$·K$^{-1}$) with a maximum at 100.0 °C (49.93 kJ·kg$^{-1}$·K$^{-1}$) and returning to the original values at a temperature of 105.0 °C. The moisture content of the wood during the tests was 14%.

Wood density affects the rate of charring and mass loss. Many authors found that charring rates decrease with increasing density (Cachim and Franssen 2009; Yang *et al*. 2009a,b; Friquin 2011; Bartlett *et al*. 2015; Schmid *et al*. 2015;). Bartlett *et al*. (2019) state that wood with higher density will char more slowly due to the greater mass of material to pyrolyze. According to that, more energy is required for endothermic reactions. Friquin (2011), Yang *et al*. (2009b) and Hugi *et al*. (2007) presented that mass loss rates increase for samples with higher density and charring rate decreases.

In materials in which a phase transformation occurs, it is important to know the temperature at which the phase transformation begins and ends. Zhang *et al*. (2020) showed that temperatures can be determined using the T-history method. The calculation was based on finding the minimum of the second derivative, the inflection points and the maximum of the first derivative. Subsequently, the intersections of the tangents from these points are determined, and the resulting two points represent the boundaries of the phase change.

Wood can be understood as an organic composite material (wood-water) due to its moisture content. As already explained, the water contained in wood has a significant effect on the material properties of the wood-water system. When the temperature of water evaporation is reached, a phase change occurs in the system, which is presented by a change in properties. The effect of water evaporation is best visible when considering the specific heat values, presented by a steep increase in values in the range from 100.0 to 120.0 °C (Fredlund 1988; Fuller *et al*. 1992; Mehaffey *et al*. 1994; König 2000; Frangi 2001; EN 1995-1-2 2004). The effect of water evaporation on thermal conductivity has not yet been further investigated (Bie *et al*. 2018). Authors investigating the values of thermal conductivity of wood at elevated temperatures made measurements outside the temperature range where phase transformation occurs (Janssens and White 1994; Frangi 2001; EN 1995-1-2 2004; Maciulaitis *et al*. 2012; Wald *et al*. 2017; Kamenická *et al*. 2018; Bartlett *et al*. 2019; Kmiecik 2019; Malaga-Tobola *et al*. 2019; Naser 2019; Hu *et al*. 2023).

There are two methods to measure the thermal conductivity during phase transitions, static and transient measurement methods such as laser flash method (LFA). LFA is commonly used to measure thermal diffusivity $\alpha$ and the thermal conductivity $\kappa$ according to Eq. 3,

$$\kappa = C \times \alpha \times \rho \tag{3}$$

where $\rho$ is the density and $C$ is the heat capacity. According to Chen *et al*. (2019), for materials with phase transition, there exists extra energy exchange to change a material's internal energy. For this purpose, they corrected thermal transport equation by including the heat exchange term to the phase transition equation to reveal how phase transition affects the measured thermal conductivity (Eq. 4),

$$\kappa \frac{\partial T}{\partial x_l} \times \Delta S - \kappa \frac{\partial T}{\partial x_r} \times \Delta S + C\rho \frac{\partial T \times \Delta S \times \Delta x}{\partial t} + \Delta H d \frac{\partial a \times \Delta S \times \Delta x}{\partial t} = 0 \tag{4}$$

where the first term is an input heat flow, the second term is an output heat flow, the third term is an absorbed heat, and the last term is the heat absorbed by phase transition. $\Delta S$ is the cross-sectional area, $\kappa$ is the thermal conductivity, $\Delta H$ is enthalpy change, $C$ is the thermal capacity, and $\rho$ is the density. Chen *et al*. (2019) also showed in different materials,

that due to the increase in temperature, a sharp change in thermal conductivity occurs during the phase change. Similar conclusions were reached by Mathur *et al*. (2021), who investigated the change in thermal conductivity during the phase change of polymers. They showed that because of the phase change, there is a significant increase in thermal conductivity, while the maximum was recorded in the middle of the temperature interval delimiting the phase change.

## EXPERIMENTAL

The methodology of the work was divided into two main parts. The first part was the performance of a medium-scale fire test of a wooden beam made of spruce wood loaded with a radiant heat source. The aim of the test was to obtain information on temperature courses inside the beam during the fire loading and to obtain information on the initial density and moisture content of the wooden beam. The second part was the creation of a FEA and simulation of this wooden beam loaded with a radiant heat source using different settings of material properties.

### Medium-Scale Fire Test

The temperature profiles over time were evaluated based on the medium-scale fire test. The medium-scale test was done with Norway spruce (lat. *Picea abies*) wooden beams, which were harvested in the Forest Enterprise territory belonging to the Technical University in Zvolen, in the central part of Slovakia during the autumn 2023. Test samples were made from the tree stem, *i.e.*, the prisms with dimensions 100 x 100 x 1,000 mm. Test samples were not dried. The average density and moisture content was determined by gravimetric method from 6 samples with dimensions of 100 x 100 x 100 mm produced from the same tree stem wood as used in the medium scale fire tests. No surface treatment was applied to the test samples. Four test samples were subjected to the medium-scale test (Fig. 1). The test specimen was placed on a structure made of aerated concrete blocks so that the loading area of the test sample was at the same height as the center axis of the radiation panel.

**Fig. 1.** Medium scale fire test

The medium-scale fire test lasted 30 min, during which the temperature courses were scanned at predetermined locations of the test sample. Temperature courses were scanned using NiCr-Ni thermocouples (Omega Engineering Inc., Norwalk, CT, USA) with a measuring range of -40.0 to +1200.0 °C. The locations of the thermocouples in the test sample are shown in Fig. 2.

A total of 10 thermocouples in 2 groups were placed in predefined locations in the middle of the sample at a depth of 50 mm for each sample. Thermocouple T1 and T6 was 10 mm depth from the exposed side, T2 and T7 20 mm, T3 and T8 40 mm, T4 and T9 60 mm, and T5 and T10 80 mm.

At the same time, one thermocouple scanned the radiation panel load concerning the location of the test sample from the radiation panel and the other thermocouple scanned the ambient temperature, which was 17.0 ± 3.0 °C during the medium-scale test. AHLBORN ALMEMO 2290-8710 V7 (Ahlborn Messund Regelungstechnik GmbH, Holzkirchen, Germ) was used to record temperatures.

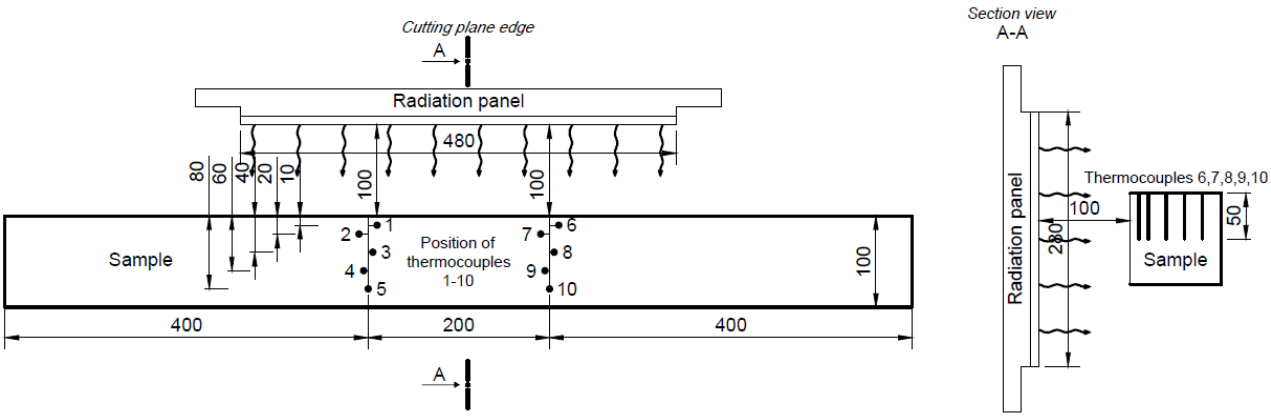


**Fig. 2.** Positions of thermocouples in samples

The test specimens were loaded with a radiation panel placed 100 mm from the test specimen. The size of the radiation surface was 480 x 280 mm. The energy source of the ceramic radiation panel was propane-butane gas at a constant flow rate 15 $m^3 \cdot h^{-1}$ with heat capacity 50 kW. During the tests, occurrences of 1 to 2 cm high laminar flames were observed at the upper edge of the samples for a period of 2 to 10 minutes. But their significance for the back heat flux to the surface of sample was very small.

A Fluke RSE600 infrared camera (Fluke Corporation, Everett, WA, U.S.) with temperature measurement range −10.0 to +1,200.0 °C was used to measure the surface temperature and a heat flux between radiation panel and sample during the tests. The infrared camera was placed on a construction above the sample at a height of 2 m. Thermal records from the infrared camera were used as an input data for the FEM.

## Finite Element Model

A preparation of the FEM that would comprehensively describe the entire combustion process and the formation of a charred layer is complicated due to many boundary conditions. It is more advantageous to simplify the model to the process of heat transfer through the material and reaching the charring temperature using thermal analysis (Frangi *et al*. 2008; Molina *et al*. 2012; Zhang *et al*. 2012; Couto *et al*. 2016; Regueira and Guaita 2018; Spilák and Majlingová 2022; Spilák *et al*. 2022a). The authors used thermal analysis and ANSYS software to study the behaviour of different timber construction

element types exposed to thermal loading. Because it is a heat transfer over time and a static result is not sought, the use of transient analysis is appropriate (Spilák and Majlingová 2022; Spilák *et al*. 2022a). For this purpose, transient thermal analysis, and software ANSYS 2023/R2 (ANSYS, Inc., Canonsburg, PA, USA) were used.

For governing the relationship between heat flux and temperature software ANSYS used the Fourier's law (Eq. 5), where $q$ is the heat flux, $\nabla T$ is the temperature gradient and $k$ is the thermal conductivity, which represents the ability of material to transfer heat by conduction. Under steady state conditions, thermal conductivity is defined as the heat flux transmitted through a material due to a unit temperature gradient. Because wood materials characteristics change with temperature, Fourier's law in a one-dimensional space is modified, where the thermal conductivity $k$ is a function of temperature $T$ (Eq. 6). Equations 4-5 do not include time for solving heat transfer problems. For solving complex 2D or 3D geometry, ANSYS software used Newton–Raphson method.

$$q = -k \cdot \nabla T \quad (5)$$

$$q = -k(T) \cdot \nabla T \quad (6)$$

The main equation for transient heat conduction through a solid is including the thermal equilibrium (Eq. 7,8).

$$k \times \left(\frac{\partial^2 T}{\partial x^2} + \frac{\partial^2 T}{\partial y^2} + \frac{\partial^2 T}{\partial z^2}\right) + q = \rho \times c \frac{\partial T}{\partial t} \quad (7)$$

$$k\nabla^2 \times T + q = \rho \times c \frac{\partial T}{\partial t} \quad (8)$$

where $\rho$ is density of a material, $c$ is specific heat capacity, $k$ is thermal conductivity, $q$ is heat flux, and $T$ is thermodynamic temperature. In the equation for transient heat conduction, the expression on the right side of the equation ($\rho \times c\ \partial T/\partial t$) represents the rate of energy storage in the body.

## Modelling the Behaviour of Structural Elements in Fire in ANSYS Software

The FEM was created in the "SpaceClaim" environment (ANSYS, Inc., Canonsburg, PA, USA) and was simplified to a simple cube with dimension of 100 mm and holes for thermocouples without supporting structures and the environmental condition. This simplification is necessary to reduce computational time of the computer model. The absence of environment and structures did not affect the simulation results.

Usually, the wooden beam is heated evenly mostly on one side of it and heat transfer perpendicular to the fibres is dominant. In such as case, the difference in results when using isotropic thermal conductivity or orthotropic thermal conductivity is negligible. Using isotropic thermal conductivity simplifies and speeds up the calculations. The "Patch Conforming Method" was applied to create a wooden beams and radiation panel mesh. The tetrahedral mesh with element size 2.5 mm was created for wooden beams, while the hexahedral mesh with element size 2.5 mm was created for the radiation panel (Fig. 3). In the holes areas "Inflation" function was used to create smoother mesh. The total number of 584,632 elements and 875,960 nodes were generated.

The connection region in the model was created manually, representing the thermal connection between the radiation panel and the thermally loaded surface of the wooden beam. The initial temperature was set to 17.0 °C based on the results of the fire tests provided. The simulation duration was set to 1,800 s, *i.e.*, 30 min. The duration of a sub-step was set to 30 s and the maximum number of iterations was 1,000 based on the previous

study (Špilák *et al.* 2022b). During the calculation process, there was no problem with convergence criterion. As a boundary condition of the simulation in ANSYS (Fig. 4a), a uniform surface radiation panel with temperature of 855.0 °C was set. The radiation panel surface temperature values were recorded by the thermal imaging camera and thermocouple when providing the real fire tests. The surface temperature of the radiation panel was approximately constant during the entire fire test (±8.0 °C).

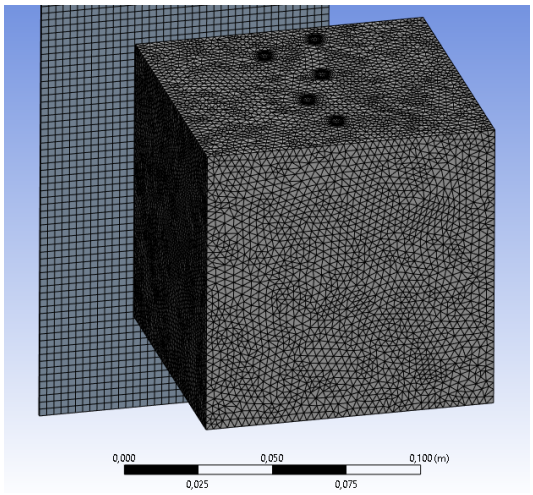


**Fig. 3.** Finite element mesh

*Method of Solution and Processing of Results*

The temperatures form the simulations were recorded by Average Temperature" function in predefined positions in holes as used in the real fire tests provided (Fig. 4b). Temperature outputs were processed into the tabular form.

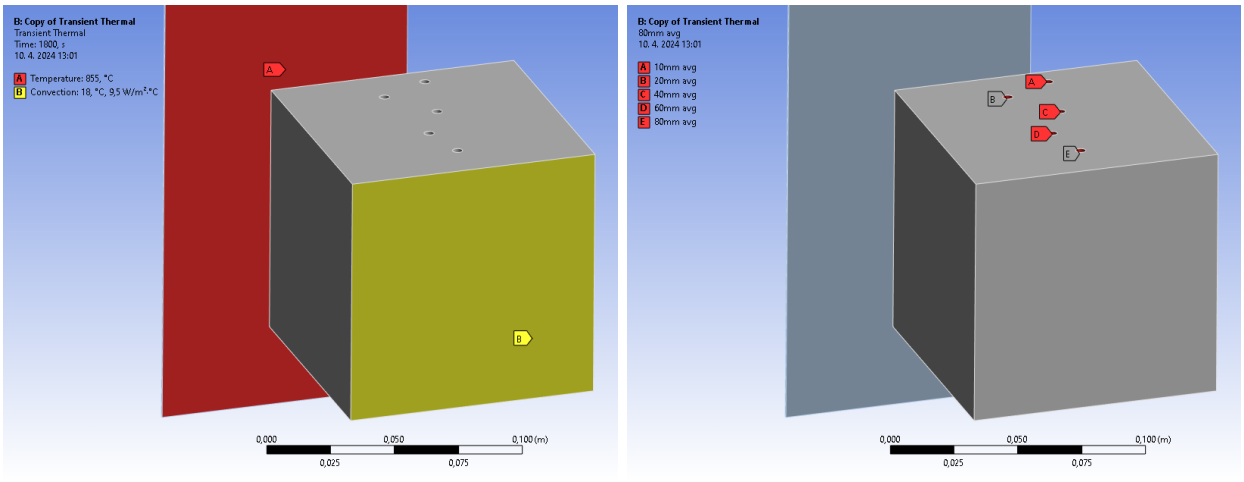


**a)** **b)**

**Fig. 4.** Prepared model: a) Boundary condition, b) Measuring of the temperature in the test sample

*Validation prepared model using the results of medium-scale fire tests*

The validation of a FEM is a process of verification of the exactitude of the models and the material characterization associated with the existing experimental results (Hietaniemi 2007). The validation of the prepared FEM was provided based on the

temperature data, which were measured by the thermocouples. The starting point for FEM validation was a comparison of results from real fire tests and simulations. The key task was to achieve the highest possible accuracy of the simulation.

*Implementation of input parameters of material characteristics*

The material characteristics of wood in combination of density, thermal conductivity, thermal capacity, and enthalpy were inserted into the created FEA model. All properties were temperature dependent. The wood density was calculated according to EN 1995-1-2 (2004). The initial density of wood was entered based on the results of density measurements using the gravimetric method. In the case of thermal conductivity of wood, several settings were used. The initial thermal conductivity curve was based on EN 1995-1-2 (2004), which was gradually modified according to Çavuş *et al*. (2019), at the phase change temperature of water, using the settings according to Chen *et al*. (2019) and Mathur *et al*. (2021). The temperatures at which the phase transformation of water in wood occurs were determined from the temperature curves obtained from medium-sized tests using the T-history method according to Zhang *et al*. (2020). MATLAB R2023b software (MathWorks, Inc., Natick, MA, USA) was used for this purpose. Enthalpy was calculated using specific heat according to Naser (2019).

## RESULTS AND DISCUSSION

The average moisture content of the wood was determined using the gravimetric method to be 9.54 % with a standard deviation of 0.23 %. The average density of wood at zero moisture content was 387.4 kg·m$^{-3}$ with a standard deviation of 11.9 kg·m$^{-3}$. At a moisture content of 9.54%, the average density of wood was 424.4 kg·m$^{-3}$ with a standard deviation of 13.9 kg·m$^{-3}$. The results from medium-scale tests of wooden beams were processed in the form of graphs; a separate graph was processed for each depth with a determined average value and standard deviation. At a depth of 1 cm, the average standard deviation was 53.4 °C, 2 cm 14.6 °C, 4 cm 2.6 °C, 6 cm 4.3 °C, and 8 cm 1.6 °C (Fig. 5).

The temperature curves show that a phase change of the water contained in the wood occurred at a depth of 1 and 2 cm. These temperature curves were used to determine the beginning and end of the phase transformation according to the T-history method according to Zhang *et al*. (2020). The average values of "Average 1 cm" and "Average 2 cm" were modified in MATLAB software using the application "Data Cleaner". The "Smooth Data" function with parameters "Local quadratic regression" with 0.08 smoothing factor was used to smooth the curve. The goal was to smooth the curves to determine the inflection points, the minimum of the second derivative and the maximum of the first derivative. Residual plots were generated for a better representation of changes in the resulting thermal curve (Fig. 6). Coefficient of determination $R^2$ had a value of 0.99996 in both cases.

Subsequently, curves of the first and second derivatives were made for temperature profiles at a depth of 1 and 2 cm, from which the minimum of the second derivative (t1), the inflection point (t2) and the maximum of the first derivative (t3) were determined using MATLAB software. For the temperature profile at a depth of 1 cm, t1 was 92.5 °C, t2 112.6 °C and t3 188.5 °C (Fig. 7c). For the temperature profile at a depth of 2 cm, t1 was 90.1 °C, t2 117.0 °C and t3 186.7 °C (Fig. 7b).

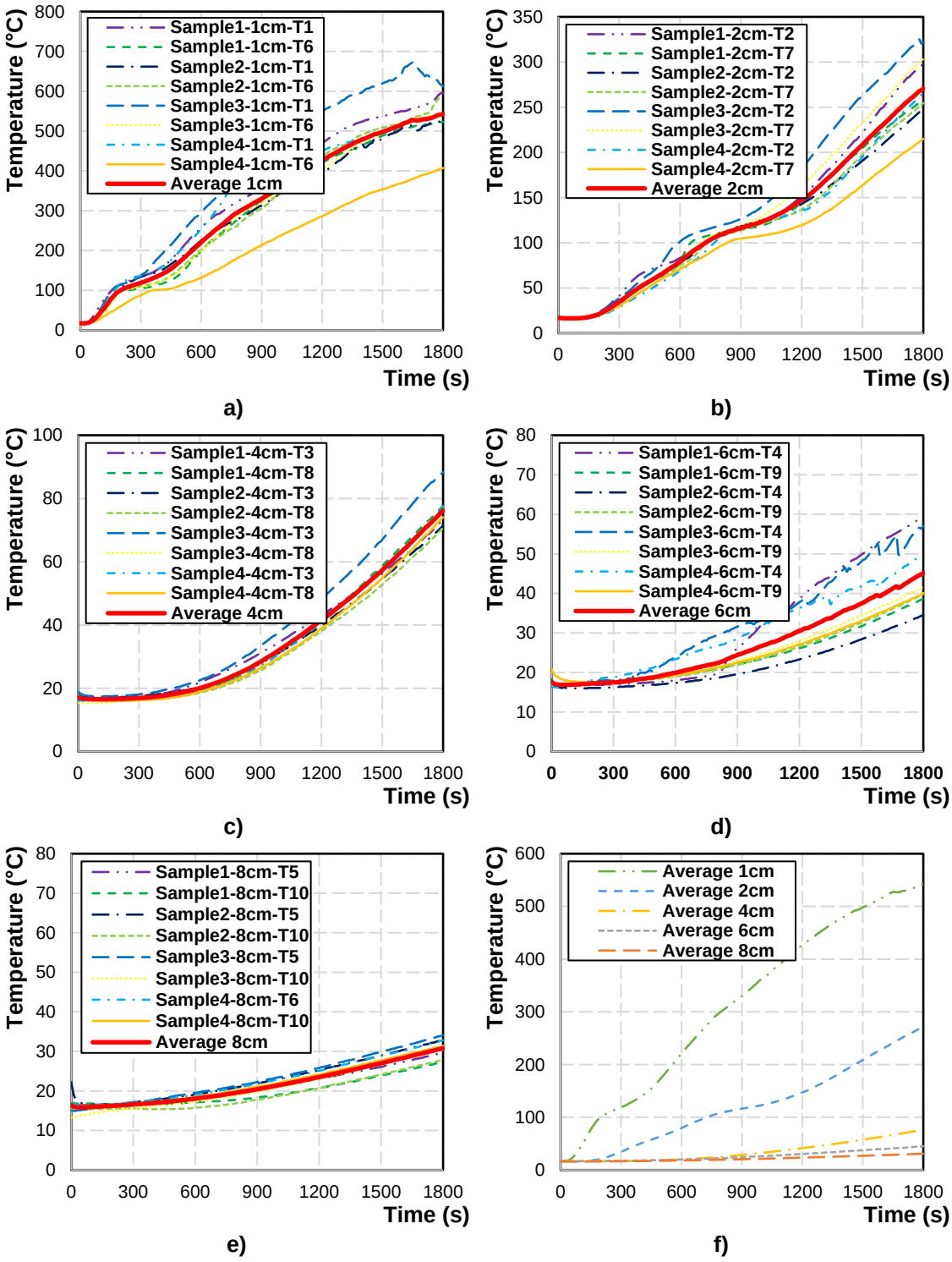


**Fig. 5.** Comparison of the time-temperature curves in the different depths: a) depth 1 cm, b) depth 2 cm, c) depth 4 cm, d) depth 6 cm, e) depth 8 cm, f) comparison of all average curves

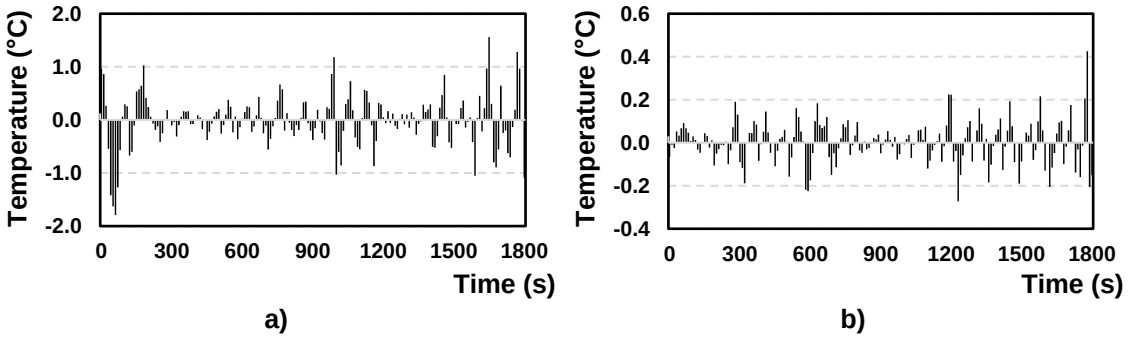


**Fig. 6.** Residuals plots of smooth data: a) Average 1 cm b) Average 2 cm

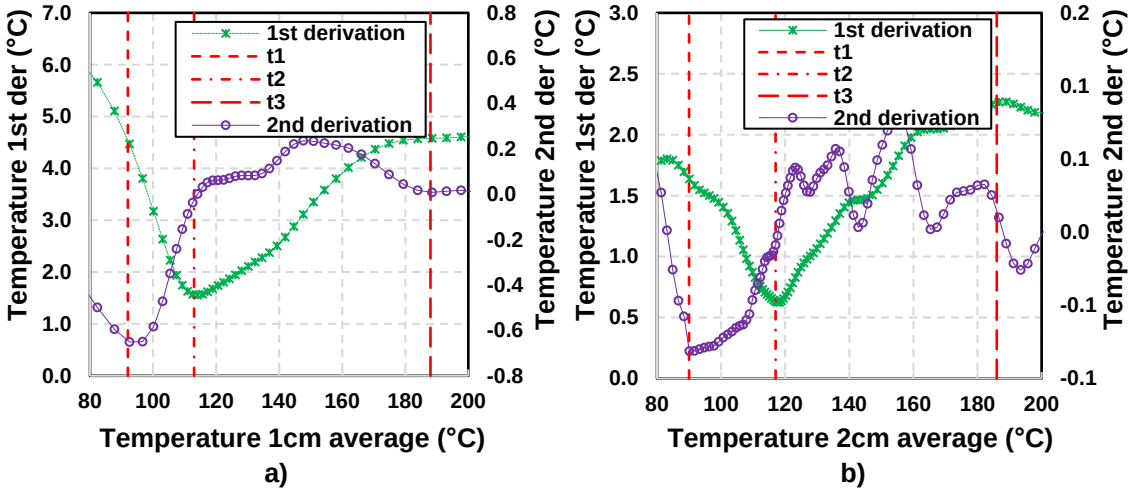


**Fig. 7.** Curves of the first and the second derivation: a) Average 1 cm b) Average 2 cm

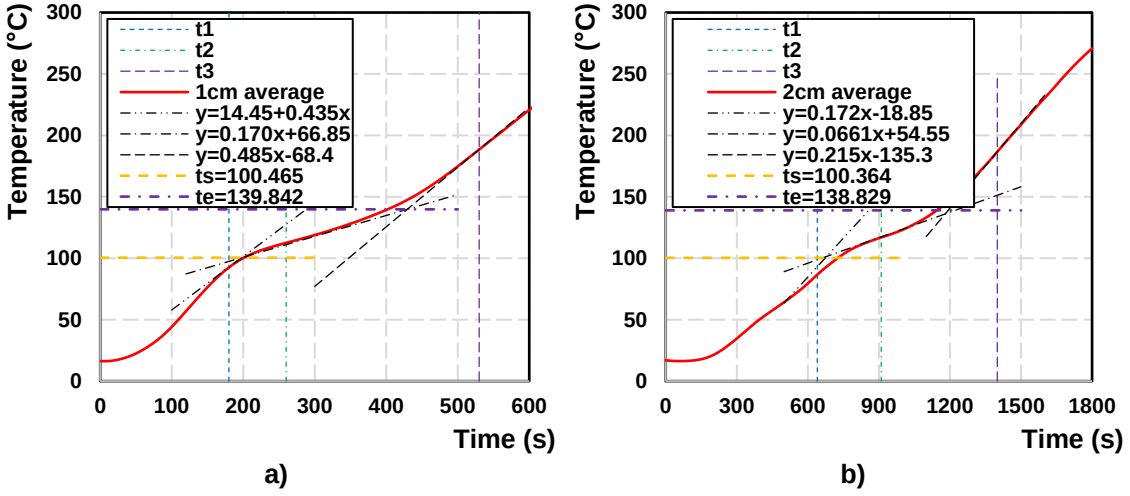


**Fig. 8.** Determination of the starting and ending points of the phase change a) Average 1 cm b) Average 2 cm

Tangents of points $y$=14.45+0.435$x$, $y$=0.170$x$+66.85, $y$=0.485$x$–68.4 for 1 cm depth and $y$=0.172$x$–18.85, $y$=0.0661$x$+54.55, $y$=0.215$x$–135.3 for 2 cm depth were generated. Using the intersections of the tangents, the temperatures of the beginning and end of the phase transformation were determined. For a depth of 1 cm, the values were determined at 100.4 and 139.8 °C (Fig. 8a). For a depth of 2 cm, the values were determined

at 100.4 and 138.8 °C (Fig. 8b). The average values were 100.4 and 139.3 °C. The determined values were used in adjusting the input values of the computer model.

Subsequently, the material characteristics of thermal conductivity, density, and enthalpy were implemented in the model (Fig. 9) (Tab. 1).

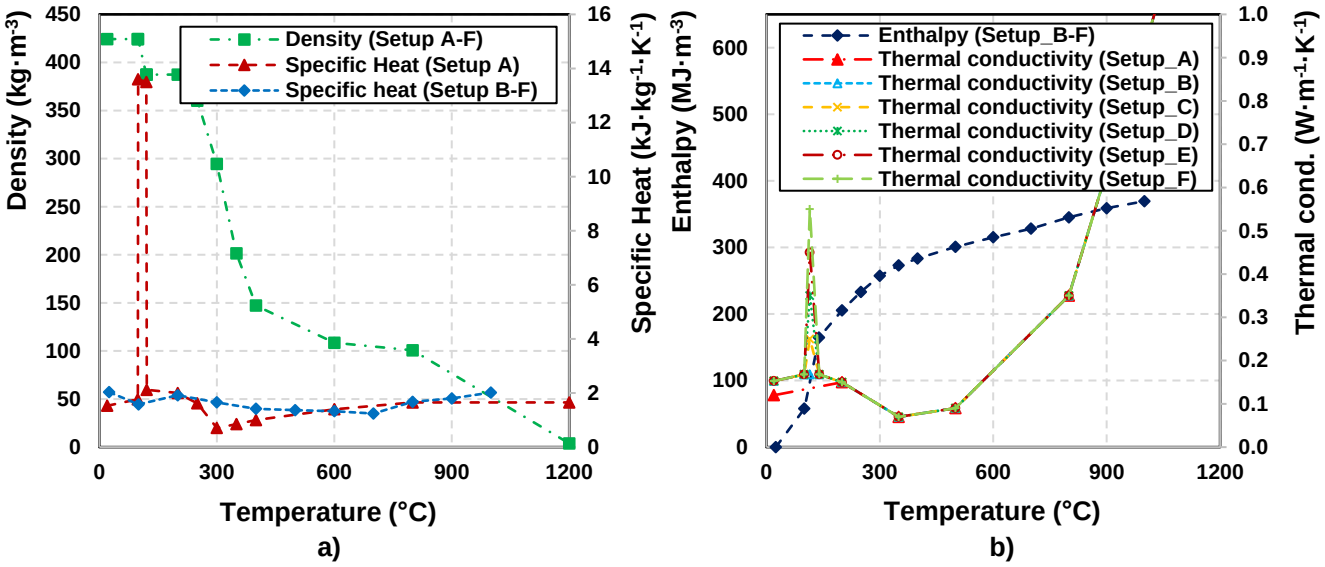


**Fig. 9.** Input data (density, specific heat, enthalpy, and thermal conductivity) in the process of computer modelling: a) density and specific heat b) enthalpy and thermal conductivity

A total of 6 different settings A–F were tried. The initial setup of A was based on EN 1995-1-2 (2004). In setups B–F, enthalpy was used, the values of which were calculated using thermal capacity according to Naser (2019). Adjustments were made for the thermal conductivity of the wood in setups B–F. First, the initial thermal conductivity of wood at a temperature of 20.0 °C and a moisture content of 9.54% was adjusted according to the Eqs. 1 and 2 to a value of 0.153 $W \cdot m^{-1} \cdot K^{-1}$. Several authors (Janssens and White 1994; Frangi 2001; EN 1995-1-2 2004; Maciulaitis *et al*. 2012; Wald *et al*. 2017; Kamenická *et al*. 2018; Bartlett *et al*. 2019; Kmiecik 2019; Malaga-Tobola *et al*. 2019; Naser 2019; Hu *et al*. 2023) report that with increasing temperature, the value of thermal conductivity increases linearly on average by approximately 0.015 $W \cdot m^{-1} \cdot K^{-1}$ at 100.0 °C. Therefore, the thermal conductivity at a temperature of 100.0 °C was set to 0.168 $W \cdot m^{-1} \cdot K^{-1}$. Different thermal conductivity setups (B-F) were tested in the phase change region. The thermal conductivity maximum was gradually changed (0.168, 0.25, 0.35, 0.45 and 0.55 $W \cdot m^{-1} \cdot K^{-1}$) in the inflection point, which was located on average at a temperature of 114.8 °C.

Density loss values were defined according to EN 1995-1-2 (2004). The enthalpy plot was created using equations (Eqs. 9 through 11).

$$H_{T_1} = H_{T_0} + c_{dw} \times \rho_{dw} \times (T_1 - T_0) + c_w \times \rho_w \times (T_1 - T_0);\ 0 < T_1 < 100.4 \quad (9)$$

$$H_{T_2} = H_{T_1} + c_{dw} \times \rho_{dw} \times (T_2 - T_1) + H_{evap} \times \rho_w;\ 100.4 \leq T_2 \leq 139.3 \quad (10)$$

$$H_{T_3} = H_{T_2} + c_{dw} \times \rho_{dw} \times (T_3 - T_2);\ 139.3 < T_3 < 1200 \quad (11)$$

where $H_{T0}$ represents the starting point of the volume enthalpy curve and is equal to 0, $c_{dw}$ is thermal capacity of a dry wood according to Naser (2019), $\rho_{dw}$ is density of the dry wood,

$c_w$ is thermal capacity of water (4.22 kJ·kg$^{-1}$·K$^{-1}$), and $\rho_w$ is density of water in wood. Equation 5 represents the calculation of the enthalpy of dry wood and the water content of the wood at temperature $T_1$. Equation 6 represents the calculation of enthalpy, when the state of water changes up to the temperature $T_2$. In this equation, $H_{evap}$ is enthalpy of evaporation (2257 kJ·kg$^{-1}$). Equation 7 represents the calculation of the enthalpy of dry wood at temperature $T_3$.

**Table 1.** Input Data

| Temp. (°C) | Density (kg·m$^{-3}$) | Specific Heat (kJ·kg$^{-1}$·K$^{-1}$) | | Thermal Conductivity (W·m$^{-1}$·K$^{-1}$) | | | | | | Enthalpy (MJ·m$^{-3}$) |
|---|---|---|---|---|---|---|---|---|---|---|
| | Setup A-F | Setup A | Setup B-F | Setup A | Setup B | Setup C | Setup D | Setup E | Setup F | Setup B-F |
| 20 | 424.4 | 1.53 | | 0.120 | 0.153 | 0.153 | 0.153 | 0.153 | 0.153 | 0 |
| 25 | 424.4 | | 2.034 | | | | | | | |
| 99 | 424.4* | 1.77 | | | | | | | | |
| 100 | 424.4* | 13.60 | 1.579 | | | | | | | |
| 100.4 | 424.4** | | | | 0.168 | 0.168 | 0.168 | 0.168 | 0.168 | 57.9 |
| 114.8 | | | | | 0.168 | 0.25 | 0.35 | 0.45 | 0.55 | |
| 120 | 387.4* | 13.50 | | | | | | | | |
| 121 | 387.4* | 2.12 | | | | | | | | |
| 139.3 | 387.4** | | | | 0.168 | 0.168 | 0.168 | 0.168 | 0.168 | 164.6 |
| 200 | 387.4 | 2.00 | 1.918 | 0.15 | 0.150 | 0.150 | 0.150 | 0.150 | 0.150 | 205.4 |
| 250 | 360.3 | 1.62 | | | | | | | | 233.0 |
| 300 | 294.4 | 0.71 | 1.654 | | | | | | | 257.4 |
| 350 | 201.4 | 0.85 | | 0.070 | 0.070 | 0.070 | 0.070 | 0.070 | 0.070 | 272.9 |
| 400 | 147.2 | 1.00 | 1.417 | | | | | | | 283.3 |
| 500 | | | 1.367 | 0.090 | 0.090 | 0.090 | 0.090 | 0.090 | 0.090 | 300.8 |
| 600 | 108.5 | 1.40 | 1.330 | | | | | | | 315.2 |
| 700 | | | 1.243 | | | | | | | 328.2 |
| 800 | 100.7 | 1.65 | 1.675 | 0.350 | 0.350 | 0.350 | 0.350 | 0.350 | 0.350 | 345.1 |
| 900 | | | 1.798 | | | | | | | 358.9 |
| 1000 | | | | | | | | | | 369.4 |
| 1200 | 3.9 | 1.65 | 2.018 | 1.500 | 1.500 | 1.500 | 1.500 | 1.500 | 1.500 | |

* Only Setup A
** Only Setup B-F

After the end of the simulations with different settings of material properties, the resulting values obtained from the simulations were compared with medium-scale fire tests (Fig. 10). The accuracy of the simulations was determined using the "Coefficient of Determination" ($R^2$) in MATLAB software.

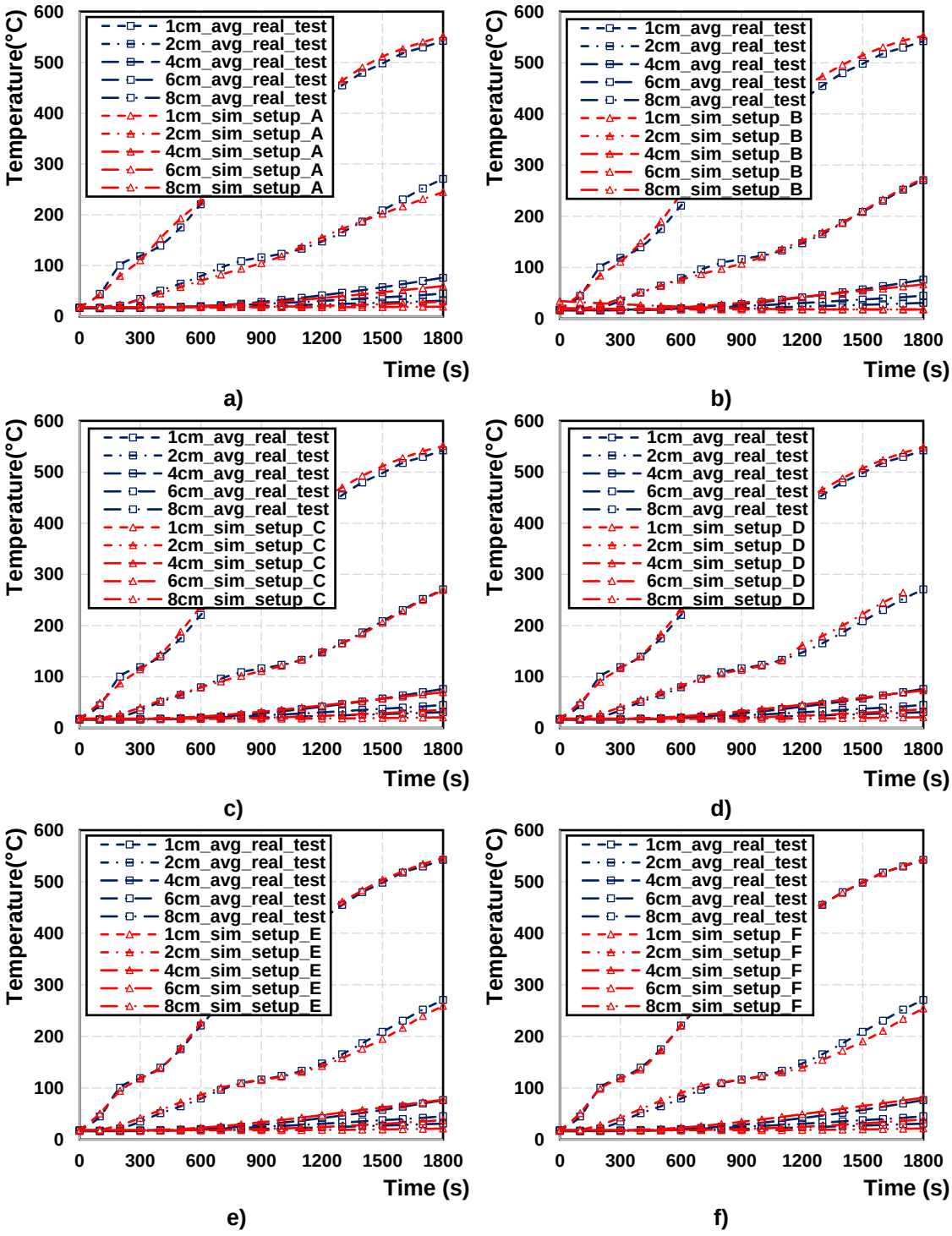


**Fig. 10.** Different setup of the computer model material characteristics: a) setup A according to EN 1995-1-2, b) setup B with enthalpy and upgrade of thermal conductivity in 20.0–100.0 °C c) setup C with upgrade of thermal conductivity with maximum value of 0.25 $W \cdot m^{-1} \cdot K^{-1}$ at 114.8 °C, d) setup D with upgrade of thermal conductivity with maximum value of 0.35 $W \cdot m^{-1} \cdot K^{-1}$ at 114.8 °C, e) setup E with upgrade of thermal conductivity with maximum value of 0.45 $W \cdot m^{-1} \cdot K^{-1}$ at 114.8 °C, f) setup F with upgrade of thermal conductivity with maximum value of 0.55 $W \cdot m^{-1} \cdot K^{-1}$ at 114.8 °C

The results of the simulations gradually show the importance of adjusting the input data (Tab. 2). With the A setup, the simulation results do not reflect the phase change starting at 100 °C. $R^2$ for setting A was 0.98257. In the case of setting B, increasing the initial thermal conductivity, and using enthalpy refined the simulation results to an $R^2$ value of 0.98444. At a temperature of 100.0 °C, a slight break representing a phase change is visible. With the C setup, the simulation results were further refined and the break in the temperature curve increased at a temperature of 100.0 °C, and $R^2$ was 0.98622. Setting D brought further refinement of the results with $R^2$ 0.98691 and highlighted the break in the temperature curve at the beginning of the phase change. Based on the setups E and F, there was an even more pronounced break at a temperature of 100.0 °C. $R^2$ was smaller and had a value of 0.98664 and 0.98588, respectively. The $R^2$ values shown represented the average $R^2$ from all depths for each setup (A–F). It is interesting to compare the accuracy of the simulation for each depth (Fig. 11).

**Table 2.** Coefficients of Determination for Different Setups

| | Setup A | Setup B | Setup C | Setup D | Setup E | Setup F |
|---|---|---|---|---|---|---|
| $R^2$ | 0.98257 | 0.98444 | 0.98622 | 0.98691 | 0.98664 | 0.98588 |

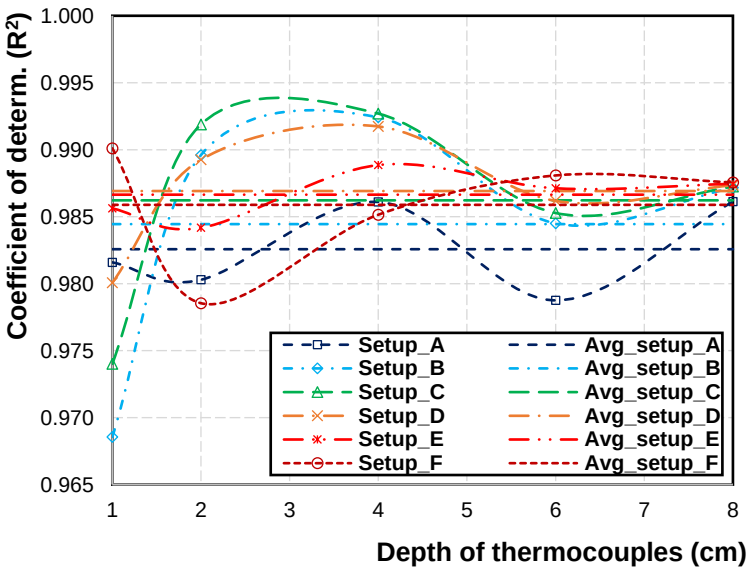


**Fig. 11.** Coefficient of determination and standard deviation depended on depth of thermocouples

Setup A produced the least accuracy with a standard deviation of 0.0028. Setup B had a standard deviation of 0.0063, C 0.0052, D 0.0030, E 0.0014, and G 0.0032. It can be seen from the graph that setting D achieved the highest accuracy, the values had an average dispersion compared to the others, which was also confirmed by the standard deviation. Settings E and F already brought lower accuracy. It follows from the results that the most accurate simulation results were obtained by setting D with a thermal conductivity value of 0.35 $W \cdot m^{-1} \cdot K^{-1}$ at a temperature of 114.8 °C with an accuracy of 98.691%.

The results show that adjusting the input settings of the material characteristics of wood can bring a significant advance in the accuracy of the results. The settings according to EN 1995-1-2 (2004) provide reliable results with relatively good accuracy, but their use in the case of different wood moistures content is limited because the input data on specific heat and thermal conductivity do not take wood moisture into account (Spilák and

Majlingová 2022). Badly set input data can lead to a high dispersion of the resulting values, which is also confirmed by Naser (2019). Regueira and Guaita (2018), Pierin *et al*. (2015), Molina *et al*. (2012), Couto *et al*. (2016), and Martínez *et al*. (2018) used in the calculation's thermal response of wood the properties of wood according to EN 1995-1-2 (2004).

Molina *et al*. (2012), who performed a numerical analysis of structural wooden elements exposed to fire with a cross section of 6 × 16 cm in ANSYS software, stated that research should focus on thermal properties data of different wood species. Due to the lack of data, the generalized data for hardwood and softwood available from technical standards (EN 1995-1-2 2004) still have to be used, which leads to inaccuracies in the numerical results of the simulation.

The most complex problem is the correct simulation of the temperature course in water phase change. Regueira and Guaito (2018) simulated this problem only partially. According to the results of Martínez *et al*. (2018), they did not simulate this range at all. Couto *et al*. (2016) used medium-scaled fire tests and FEA to examine the fire resistance of cellular wooden slabs and state that many differences between experimental and numerical results may be due to different levels of moisture content in the wood material. With the use of enthalpy, it is possible to imitate to a certain extent the phase transformation of water in wood at a temperature of 100 °C (Spilák and Majlingová 2022; Spilák *et al*. 2022a,b), which was also confirmed by the results of simulations. However, with only the help of enthalpy, the accuracy of the simulations during the phase change can be judged as average.

The T-history method (Zhang *et al*. 2020) proved to be a useful tool with which the accuracy of the simulations was highly refined. It made it possible to define the beginning and end of the phase transformation, which is strictly specified by EN 1995-1-2 (2004) but also by many other authors (Fredlund 1988; Fuller *et al*. 1992; Mehaffey *et al*. 1994; König 2000; Frangi 2001). Further refinement of the results brought an increase in the thermal conductivity of wood according to the density and moisture content in the area before the water phase change (Çavus *et al*. 2019; Špilák *et al*. 2022b). In the area of phase change of water, setting D with a thermal conductivity value of 0.45 $W \cdot m^{-1} \cdot K^{-1}$ at a temperature of 114.8 °C was shown to be the best with an accuracy of 98.691% with an almost perfect imitation of the temperature course during the phase change of water. The reason why the temperature course in the phase change area was imitated by changing the thermal conductivity is in the equations used by FEA. If a change in properties such as enthalpy, specific heat, or density of wood does not cause a change in the temperature course, the last property by which the effect of phase transformation can be imitated is the thermal conductivity, which is also confirmed by the results of authors investigating phase transformations of materials (Chen *et al*. 2019; Mathur *et al*. 2021). The results of the simulations also show that there could be a correlation between the moisture content of the wood and the maximum value of the thermal conductivity of the wood in the phase change of water.

The correct implementation of input data, especially thermal conductivity, has a significantly important influence on the simulation of a formation of charred layer and layer of degraded wood parameters, and on determining the fire resistance of wooden structural elements. According to many authors (Gerhards 1982; Östman 1985; Glos and Henrici 1991; Janssens and White 1994; König 2000; EN 1995-1-2 2004; Jong and Clancy 2004; König 2005; Van Zeeland *et al*. 2005; White and Dietenberger 2010; Naser 2019), the strength of wood in pressure and modulus of elasticity decreases dramatically with the

temperature rising in temperatures range 20.0 to 300 °C, from the maximum values to almost zero.

In the simulations, the accuracy varies depending on the thermal conductivity setting. Martinez *et al*. (2018) and Zhang *et al*. (2012) stated that the accuracy of the simulation decreased with increasing distance of the thermocouple position from the radiation panel. They further stated that it is necessary to examine the influence of water evaporation, mass transfer, pyrolysis, thermal properties of contacts between individual layers of wood and cracks formed in the wood during the thermal load.

Improving the accuracy of computer models in the field of water phase change is very important. Thanks to the refinement of the computer models and input data, it is possible to predict with better accuracy an ignition time, activation energy, and fire resistance of wood and wood-based constructions. Increasing the accuracy of computer models also improves the economics of the construction, thanks to more efficient design processes. To further improve computer models of heat transfer in wood, it is necessary to focus on the effect of moisture content on thermal conductivity of wood and its experimental determination.

## CONCLUSIONS

1. Settings according to EN 1995-1-2 (2004) provide reliable results with relatively good accuracy, but their use in the case of different wood moisture content is limited.
2. With the use of enthalpy, it is possible to imitate to a certain extent the phase transformation of water in wood at a temperature of 100.0 °C. However, with only the help of enthalpy, the accuracy of the simulations during the phase change is relatively average.
3. The T-history method is a useful tool with the help of which the accuracy of the simulations is highly accurate.
4. In the area of phase change of water, the setting with a thermal conductivity value of 0.35 $W \cdot m^{-1} \cdot K^{-1}$ at a temperature of 114.8 °C was shown to be the best with an accuracy of 98.691% with an almost perfect imitation of the temperature course during the phase change of water.
5. The results of the simulations show that there could be a correlation between the moisture content of the wood and the maximum value of the thermal conductivity of the wood in the phase change of water.

## ACKNOWLEDGMENTS

This research was funded by the Slovak Research and Development Agency, grant number APVV-SK-CN-21-0002 (40%) and APVV-22-0030 (20%). This work was supported by the Scientific Grant Agency of the Ministry of Education, Research, Development and Youth of the Slovak Republic and the Slovak Academy of Sciences under the Contract VEGA no. 1/0115/22 A comprehensive approach to the study of changes in fire parameters using progressive analytical and testing methods (20%). This publication is also the result of the project implementation: Progressive research of

performance properties of wood-based materials and products (LignoPro); ITMS 313011T720, supported by the Operational Programme Integrated Infrastructure (OPII) funded by the ERDF (20%).

## REFERENCES CITED

Acuña-Alegri, L., Salinas-Lintz, C., Sepulveda-Villarroel, V., Vasco-Calle, D., and Ananías, R. A. (2018). "Inverse determination of thermal conductivity in wood of *Pinus rathata*," *Maderas-Ciencia Y Tecnologia* 20(4), 595-610.

Amel, L., Zerizer, A., Quenard, D., Hebert, S., and Abdelkrim, C. (2016). "Experimental thermal characterization of bio-based materials (Aleppo Pine wood, cork and their composites) for building insulation," *Energy and Buildings* 116.

Bartlett, A., Hadden, R., Bisby, L., and Law, A. (2015). "Analysis of cross-laminated timber upon exposure to non-standard heating conditions," in: *Fire and Materials Conference*, San Francisco, USA.

Bartlett, A. I., Hadden, R. M., and Bisby, L. A. (2019). "A review of factors affecting the burning behaviour of wood for application to tall timber construction," *Fire Technology* 55(1), 1-49.

Bie, Y., Li, M., Malekian, R., Chen, F., Feng, Z. K., and Li, Z. X. (2018). "Effect of phase transition temperature and thermal conductivity on the performance of latent heat storage system," *Applied Thermal Engineering* 135, 218-227.

Blass, H., and Eurofortech. (1995). *Timber Engineering : STEP 1 : Basis of Design, Material Properties, Structural Components and Joints*, Centrum Hout Almere, The Netherlands, Almere, The Netherlands.

Cachim, P. B., and Franssen, J.-M. (2009). "Comparison between the charring rate model and the conductive model of Eurocode 5," *Fire and Materials* 33(3), 129-143.

Cachim, P. B., and Franssen, J.-M. (2010). "Assessment of Eurocode 5 charring rate calculation methods," *Fire Technology* 46(1), 169-181.

Çavus, V., Sahin, S., Esteves, B., and Ayata, Ü. (2019). "Determination of thermal conductivity properties in some wood species obtained from Turkey," *BioResources* 14(3), 6709-6715.

Chen, H. Y., Yue, Z. M., Ren, D. D., Zeng, H. R., Wei, T. R., Zhao, K. P., Yang, R. G., Qiu, P. F., Chen, L. D., and Shi, X. (2019). "Thermal conductivity during phase transitions," *Advanced Materials* 31(6), Article no. 1806518. DOI: 10.1002/adma.201806518

Couto, D. L. P., Fonseca, E. M. M., Piloto, P. A. G., Meireles, J. M., Barreira, L. M. S., and Ferreira, D. (2016). "Perforated cellular wooden slabs under fire: Numerical and experimental approaches," *Journal of Building Engineering* 8, 218-224.

EN 1995-1-2 (2004). "Eurocode 5: Design of timber structures - Part 1-2: General - Structural fire design," European Committee for Standardization, Brussels, Belgium.

Frangi, A. (2001). "Brandverhalten von Holz-Beton-Verbunddecken," *ETH Zurich*; 2001. https://www.research-collection.ethz.ch/bitstream/handle/20.500.11850/145666/eth-24596-01.pdf.

Frangi, A., Erchinger, C., and Fontana, M. (2008). "Charring model for timber frame floor assemblies with void cavities," *Fire Safety Journal* 43(8), 551-564.

Fredlund, B. (1988). *A Model for Heat and Mass Transfer in Timber Structures During Fire: A Theoretical, Numerical and Experimental Study*, [Doctoral Thesis

(monograph), Division of Fire Safety Engineering]. Lund University, Department of Fire Safety Engineering.

Friquin, K. L. (2011). "Material properties and external factors influencing the charring rate of solid wood and glue-laminated timber," *Fire and Materials* 35(5), 303-327. DOI: 10.1002/fam.1055

Fuller, J. J., Leichti, R. J., and White, R. H. (1992). "Temperature distribution in a nailed gypsum-stud joint exposed to fire," *Fire and Materials* 16(2), 95-99. DOI: 10.1002/fam.810160206

Gerhards. (1982). "Effect of moisture content and temperature on the mechanical properties of wood: an analysis of immediate effects," *Wood Fiber Sci.* 14(1), 4–36. https://wfs.swst.org/index.php/wfs/article/view/501.

Glos, P., and Henrici, D. (1991). "Längsdruck-E-Modul von Fichtenbauholz im Temperaturbereich bis 150 °C," *European Journal of Wood and Wood Products*, 49, 298-298.

Harper, C. A. (2003). *Handbook of Building Materials for Fire Protection*, McGraw Hill LLC.

Hietaniemi, J. (2007). "Probabilistic simulation of fire endurance of a wooden beam," *Structural Safety* 29(4), 322-336.

Hu, Y. P., Li, W. B., Wu, S., Wang, Y. J., Zhong, W. Z., and Zhang, H. (2023). "Experimental study of the anisotropic thermal conductivity of spruce wood," *International Journal of Thermophysics* 44(8).

Hugi, E., Wuersch, M., Risi, W., and Ghazi Wakili, K. (2007). "Correlation between charring rate and oxygen permeability for 12 different wood species," *Journal of Wood Science* 53(1), 71-75.

Jang, E. S., and Kang, C. W. (2022). "The relationship between bulk density and thermal conductivity in various Korean woods," *Wood Research*, 67(2), 178-186.

Janssens, M. L., and White, R. H. (1994). "Short communication: Temperature profiles in wood members exposed to fire," *Fire and Materials* 18(4), 263-265.

Jong, F., and Clancy, P. (2004). "Compression properties of wood as functions of moisture, stress and temperature," *Fire and Materials* 28, 209-225.

Kamenická, Z., Sandanus, J., Blesák, L., Cabová, K., and Wald, F. (2018). "Methods for determining the charring rate of timber and their mutual comparison," *Wood Research* 63(4), 583-590.

Kmiecik, K. (2019). "Impact of wood species on the timber beam strength and stiffness under fire," *IOP Conference Series: Materials Science and Engineering* 586(1), 012004.

König, J. (2000). "Timber frame assemblies exposed to standard and parametric fires. Part 2 A design model for standard fire exposure," 76. Retrieved from https://urn.kb.se/resolve?urn=urn:nbn:se:ri:diva-28624

König, J. (2005). "Structural fire design according to Eurocode 5—design rules and their background," *Fire and Materials* 29, 147-163.

Kristák, L., Igaz, R., and Ruziak, I. (2019). "Applying the EDPS method to the research into thermophysical properties of solid wood of coniferous trees," *Advances in Materials Science and Engineering*.

Maciulaitis, R., Jefimovas, A., and Zdanevicius, P. (2012). "Research of natural wood combustion and charring processes," *Journal of Civil Engineering and Management* 18(5), 631-641.

Malaga-Tobola, U., Lapka, M., Tabor, S., Nieslony, A., and Findura, P. (2019). "Influence

of wood anisotropy on its mechanical properties in relation to the scale effect," *International Agrophysics* 33(3), 337-345.

Maraveas, C., Miamis, K., Matthaiou, C. E., and Maraveas, C. (2015). "Performance of timber connections exposed to fire: A review," *Fire Technology* 51(6), 1401-1432.

Martinez-Martinez, J. E., Alonso-Martinez, M., Rabanal, F. P. A., and Del Coz Diaz, J. J. (2018). "Study of the influence of heat transfer of a CLT beam through FEM," *IOP Conf. Series: Journal of Physics*: 1107 (2018) 032003. DOI: 10.1088/1742-6596/1107/3/032003

Mathur, V., Arya, P. K., and Sharma, K. (2021). "Estimation of activation energy of phase transition of PVC through thermal conductivity and viscosity analysis," in: *International Conference on Innovations in Technology, Management and Design for Achieving Sustainable Development Goals - Materials Science (ICSDG)*, Jaipur, India, pp. 1237-1240.

Mehaffey, J. R., Cuerrier, P., and Carisse, G. (1994). "A model for predicting heat transfer through gypsum-board/wood-stud walls exposed to fire," *Fire and Materials* 18(5), 297-305.

Molina, J., Calil, C., Kimura, E., Pinto, E., Regobello, R., Scheer, M., Carneiro, C., Bressan, O., and Santos, K. (2012). "Análise numérica do comportamento de elementos de madeira em situação de incêndio," *Floresta e Ambiente* 19, 162-170.

Mvondo, R. R. N., Damfeu, J. C., Meukam, P., and Jannot, Y. (2020). "Influence of moisture content on the thermophysical properties of tropical wood species," *Heat and Mass Transfer* 56(4), 1365-1378.

Naser, M. Z. (2019). "Properties and material models for common construction materials at elevated temperatures," *Construction and Building Materials* 215, 192-206.

Östman, B. (1985). "Wood tensile strength at temperatures and moisture contents simulating fire conditions," *Wood Science and Technology* 19, 103-116.

Pecenko, R., Svensson, S., and Hozjan, T. (2015). "Modelling heat and moisture transfer in timber exposed to fire," *International Journal of Heat and Mass Transfer* 87, 598-605. DOI: 10.1016/j.ijheatmasstransfer.2015.04.024

Peng, L., Hadjisophocleus, G., Mehaffey, J., and Mohammad, M. (2011). "Predicting the fire resistance of wood–steel–wood timber connections," *Fire Technology* 47(4), 1101-1119. DOI: 10.1007/s10694-009-0118-4.

Pierin, I., Silva, V. P., and Rovere, H. L. L. (2015). "Thermal analysis of two-dimensional structures in fire," *Revista IBRACON de Estruturas e Materiais* 8(1), 25-36.

Pinto, E., Machado, G. O., Felipetto, R. P. F., Christoforo, A. L., Rocco Lahr, F., and Calil, C. (2016). "Thermal degradation and charring rate of and wood species," *The Open Construction and Building Technology Journal* 10, 450-456.

Regueira, R., and Guaita, M. (2018). "Numerical simulation of the fire behaviour of timber dovetail connections," *Fire Safety Journal* 96, 1-12. DOI: 10.1016/j.firesaf.2017.12.005.

Reszka, P., and Torero, J. L. (2008). "In-depth temperature measurements in wood exposed to intense radiant energy," *Experimental Thermal and Fluid Science* 32(7), 1405-1411.

Richter, F., and Rein, G. (2020). "A multiscale model of wood pyrolysis in fire to study the roles of chemistry and heat transfer at the mesoscale," *Combustion and Flame* 216, 316-325. DOI: 10.1016/j.combustflame.2020.02.029.

Rinta-Paavola, A., Sukhomlinov, D., and Hostikka, S. (2023). "Modelling charring and burning of spruce and pine woods during pyrolysis, smoldering and flaming," *Fire*

*Technology* 59(5), 2751-2786. DOI: 10.1007/s10694-023-01458-9.

Shen, D. K., Fang, M. X., Luo, Z. Y., and Cen, K. F. (2007). "Modeling pyrolysis of wet wood under external heat flux," *Fire Safety Journal* 42(3), 210-217. DOI: 10.1016/j.firesaf.2006.09.001

Schmid, J., Just, A., Klippel, M., and Fragiacomo, M. (2015). "The reduced cross-section method for evaluation of the fire resistance of timber members: Discussion and determination of the zero-strength layer," *Fire Technology* 51(6), 1285-1309.

Spilák, D., and Majlingová, A. (2022). "Progressive methods in studying the charred layer parameters change in relation to wood moisture content," *Polymers*, 14(22).

Spilák, D., Majlingová, A., Kacíková, D., and Tischler, P. (2022a). "Determining the charred layer of wooden beams with finite element analysis based on enthalpy approach," *Buildings* 12(7).

Špilák D., Majlingová A., and Kačíková D. (2022b). *Progressive Methods for Determining the Fire Resistance of Wooden Beams,* Aleš Čeněk, 162.

Su, H. C., Tung, S. F., Tzeng, C. T., and Lai, C. M. (2019). "Variation in the charring depth of wood studs inside wood-frame walls with time in a fire," *Wood Research* 64(3), 449-459.

Van Zeeland, I., Salinas, J., and Mehaffey, J. (2005). "Compressive strength of lumber at high temperatures," *Fire and Materials* 29, 71-90. DOI: 10.1002/fam.871

Vololonirina, O., Coutand, M., and Perrin, B. (2014). "Characterization of hygrothermal properties of wood-based products - Impact of moisture content and temperature," *Construction and Building Materials* 63, 223-233.

Wald, F., Pokorný, M., Horová, K., Hejtmánek, P., Najmanová, H., Benýšek, M., Kurejková, M., Schwarz, I., and fakulta, Č. v. u. t. v. P. S. (2017). *Modelování Dynamiky Požáru v Budovách*, České vysoké učení technické v Praze.

White, R. H., and Dietenberger, M. (2010). "Fire safety of wood construction," *Forest Products Laboratory. Wood Handbook- Wood as an Engineering Material*, 1-17.

Yang, T. H., Wang, S. Y., Tsai, M. J., and Lin, C. Y. (2009a). "The charring depth and charring rate of glued laminated timber after a standard fire exposure test," *Building and Environment* 44(2), 231-236.

Yang, T. H., Wang, S. Y., Tsai, M. J., and Lin, C. Y. (2009b). "Temperature distribution within glued laminated timber during a standard fire exposure test," *Materials & Design* 30(3), 518-525.

Zhang, J., Xu, Q. F., Xu, Y. X., Wang, B., and Shang, J. X. (2012). "A numerical study on fire endurance of wood beams exposed to three-side fire," *Journal of Zhejiang University-Science A* 13(7), 491-505.

Zhang, Y. Y. C., Zhang, X. L., Xu, X. F., and Lu, M. Y. (2020). "Derivation of thermal properties of phase change materials based on T-history method," *Journal of Energy Storage* 27. DOI: 10.1016/j.est.2019.101062

Zvicevicius, E., Raila, A., Cipliene, A., and Ziura, K. (2019). "Influence of moisture on osier willow chops characteristics," in: *18th International Scientific Conference on Engineering for Rural Development (ERD)*, Jelgava, Latvia, pp. 1561-1567.

Article submitted: September 24, 2024; Peer review completed: November 23, 2024; Revised version received and accepted: November 23, 2024; Published: December 9, 2024.
DOI: 10.15376/biores.20.1.1230-1250